

# Co-Simulation Framework For Network Attack Generation and Monitoring

Oceane Bel, Joonseok Kim, William J Hofer, Manisha Maharjan, Sumit Purohit, Shwetha Niddodi

**Abstract**—Resilience assessment is a critical requirement of a power grid to maintain high availability, security, and quality of service. Most grid research work that is currently pursued does not have the capability to have hardware testbeds. Additionally, with the integration of distributed energy resources, the attack surface of the grid is increasing. This increases the need for reliable and realistic modeling techniques that are usable by the wider research community. Therefore, simulation testbeds have been used to model a real-world power grid topology and measure the impact of various perturbations.

Existing co-simulation platforms for powergrid focus on a limited components of the overall system, such as focusing only on the dynamics of the physical layer. Additionally a significant number of existing platforms need specialized hardware that may be too expensive for most researchers. Finally, not many platforms support realistic modeling of the communication layer, which requires use of Supervisory Control and Data Acquisition communication protocol such as DNP3 while modeling cybersecurity scenarios.

We present Network Attack Testbed in [Power] Grid (NATI[P]G), (pronounced *natig*), a standalone, containerized, and reusable environment to enable cyber analysts and researchers to run different cybersecurity and performance scenarios on powergrid. Our tool combines GridLAB-D, a grid simulator, HELICS, a co-simulation framework, and NS-3, a network simulator, to create an end-to-end simulation environment for the power grid. We demonstrate use cases by generating a library of datasets for several scenarios. These datasets can be used to detect cyberattacks at the cyber layer, and develop counter measures to these adverse scenarios.

## I. INTRODUCTION

Cyber-physical systems (CPS), such as microgrids, are key infrastructure components that impact social, financial, and national security on a daily basis. Thus, with cyberattacks increasing in sophistication by the day, there is a need to understand various failure scenarios and plan for mitigation strategies for a reliable and resilient power grid operation [1], [2]. Simulation environments have been extensively used to model CPS components, topologies, adversaries, attack sequences, and their impact on the systems [3], [4]. CPSs are complex and interdependent systems, with both discrete and continuous measurements. However, existing attack detection

The research described in this paper is part of the Resilience Through Data-Driven, Intelligently Designed Control (RD2C) Initiative at Pacific Northwest National Laboratory. It was conducted under the Laboratory Directed Research and Development Program at PNNL, a multiprogram national laboratory operated by Battelle for the U.S. Department of Energy.

O. Bel, W. Hofer, M. Maharjan, S. Purohit and S. Niddodi are with Pacific Northwest National Laboratory, Richland, WA, 99352, USA (e-mail: {obel@pnnl.gov, william.hofer, manisha.maharjan, sumit.purohit, shwetha.niddodi}@pnnl.gov).

J.-S. Kim is with the National Security Sciences Directorate, Oak Ridge National Laboratory, Oak Ridge, TN 37830, USA (e-mail: kimj1@ornl.gov).

models, such as data-driven intrusion detection and prevention systems, require high amount of data to train models before they are deployed on the grid. This stymies efforts to combat the rate of improvement that cyberattackers have when attacking Cyber-physical systems.

To develop adequate defenses, we must efficiently generate end-to-end models of systems and adversaries. Current simulators, such as NetSim [5] and Mininet [6], provide a partial view of the system, but fail to exhibit physical constraints and conditional operations across different components. Co-simulation environments have been developed to address these limitations, but struggle to address usability and flexibility challenges. Additionally, the co-simulators provide little or no support for *perturb-and-observe* to model adversarial scenarios and generate benchmark datasets for downstream applications such as risk assessment, attack detection, and risk mitigation.

We present Network Attack Testbed in [Power] Grid (NATI[P]G), a co-simulation environment for distribution power grid network using state-of-the-art simulators. This co-simulator is used to generate attack scenarios that can enable researchers to understand how attackers could behave in a network given a set of goals. Our work builds upon past work where researchers modeled attacks using network simulators to understand the behavior of attackers [7], [8]. By modeling potential adversary behaviors, researchers can develop faster ways to identify them on the network during attacks.

We focus on man-in-the-middle attacks on a power grid as our primary attack scenario. We implemented these attacks on the NS3 network simulator and measure their impact in the GridLAB-D simulator. We do not limit our scenarios to transport and session layers, but rather demonstrate application layer perturbations in the communication layer. The goal is to provide an example on how our tool can be used by other researchers without specialized hardware. Using our testbed, we identified different behaviors between grid following and grid forming inverters during cyberattacks. We also use our testbed to find settings for capacitors and generators to minimize frequency deviation when switches are tripped and microgrids are islanded.

The contributions of the paper are as follows:

- Our co-simulation tackles the entire stack, creating a simulation close to what is expected of a real test bed.
- We produce a containerized framework for a wide range of cyber resilience assessment applications, improving upon existing testbeds.
- We demonstrate the feasibility of modeling, simulating, and validating CPS environments without using special-

ized hardware.

- We leverage application layer commands using DNP3 protocol in NS3 to simulate realistic grid behaviour.
- We simulate man-in-the-middle scenarios using DNP3 protocols.

This paper is organized as follows. In Section 2, we survey existing approaches and address our motivation. Section 3 delineates the design of our framework and use cases of cyberattacks. Section 4 describes the details of attack scenarios to demonstrate the usability of our framework. We report our experimental results in Section 5. Section 6 concludes our work and discusses future work.

## II. BACKGROUND AND RELATED WORK

The power grid is a critical infrastructure due to its effect on daily life [9]. Energy providers must balance supply with demand and handle unforeseen events, such as extreme weather patterns. These events can affect the functionality of the grid and impact a large portion of the population. Any threats to the grid should be identified early enough so that providers can deal with the threats before they impact the functions of the grid [10].

In recent years, traditional power systems have become more integrated with information and communication technology, which has given way to Cyber-Physical Power Systems [11]. Alongside the growth of network simulators, more researchers are turning to simulators to develop new technology. This means that simulators must evolve to get closer to realistic networks without losing simulation efficiency.

### A. NS3

Network Simulator 3 (NS3) [12] is a network simulator commonly used in network architecture and system development. It can simulate almost all aspects of a network, including the physical properties of signal transmission. This allows users greater control over the different aspects of the network, allowing them to simulate various attack scenarios with different network topologies, interject data flows at a particular node, and replace normal data with false data. An example of this control is setting whether or not a packet has reached its final destination. This simulates how an attacker can stop a packet at the node controlled by them before sending out a new packet with different information to a victim node. Another example is updating a source IP to the original source IP that was used by the intercepted packet, leaving a victim unaware of an IP change.

Using the simulator, we can create datasets and a system that can be used by other researchers to model potential attacks. Our system has a configuration file that can be used to set different topologies and tune attack parameters. The simulator can also collect performance and routing information using NS3 monitors. The monitored information can be used to create attacker models that can be used as controllers in a network to adapt the network settings in response to attackers.

### B. GridLAB-D

GridLAB-D is a simulation tool that enables power distribution system simulation and analysis [13]. It is extensively

used to represent the system behavior of different power system components and complex interactions between these components and modern grid technologies like distributed energy resources (DERs). It can perform power flow analysis and dynamic studies and generates detailed load and market models. With the recent interests in studies regarding the interaction of power system and communication networks, GridLAB-D has been used for bench-marking IEEE feeder models for modeling detailed and dynamic power system operations, and time-series power flow simulations [14], [15]. It facilitates larger simulations of power system models and simplified implementation of system architectures for illustrating a wide range of scenarios that reflect the impacts of communication layers on power system operations.

### C. Co-simulation Environment

There are existing platforms that simulate power systems. One of these platforms [16] includes a mechanism that uses NS3 as a networking interface in conjunction with Framework for Network Co-Simulation (FNCS) and GridLAB-D as tools to keep track of value changes over time of power system components. In line with this work, we utilize a co-simulation to simulate cyberattacks on power networks. Additionally, our tool allows for larger simulation by using HELICS instead of FNCS as the interconnect between GridLAB-D and NS3. Battarai et al. [14] presents a HELICS based co-simulation environment, but the work does not focus on scenarios involving application layer perturbations. We introduce DNP3 protocol as part of NS3 to send measurement data and control commands between the NS3 nodes representing components in SCADA systems.

### D. Reconfigurable networks

Current networks have the ability to reconfigure themselves as workloads and needs change. Several things can happen during reconfiguration, such as user equipment changing which antenna it connects to or topology changes. Slicing, in 5G networks, is another way to implement reconfiguration, where partitioning the network can be done to isolate network attacks. This prevents an attacker from harming the entire network and spreading its influence. Slices can be updated as needed over time to isolate network sections or to distribute resources in response to a metric such as performance or monetary spending. Therefore, live reconfiguration can be a powerful tool for security and for enhancing performance enhancement of networks. A current research area revolves around how to make use of 5G network slicing and reconfigurability for power grids.

### E. DNP3 protocol

DNP3 is a protocol used to send packets between nodes, commonly in a utility distribution network [17]. According to surveys, more than 75% of North American electric utilities use or have used DNP3 as a communication protocol [18]. Using this protocol in conjunction with the NS3 simulator allowed us to develop an end-to-end power grid traffic simulator.

Using this setup, we can simulate different situations, such as downed nodes or attacks on the network. We can also monitor the traffic flow between the nodes to model any changes in the traffic between when the attack is happening and when the traffic is normal.

#### F. Cybersecurity simulations platforms

Previous work has been done with the goal of generating cyber attacks, such as man-in-the-middle attacks on LAN wireless network [19], WAN networks [20], hard connected [21] and VANET networks [22]. Additionally, researchers have looked at the effect of cyberattacks, like man-in-the-middle and denial of service, on power systems, and have found that denial of service attacks has significant impacts on the run time of devices on the network [23]. We focus on creating a lightweight simulation tool that can be used by other researchers. The tool can be used to parameterize the attack that they want to simulate and get traffic information characterizing the effect of the attack on the grid. Another example of attack generation platform is GridSTAGE [24], which can be used to simulate false data injection attacks. It provides a framework where the user can input the parameters of an attack, and measure its effects on network traffic.

### III. CO-SIMULATION DESIGN

This section briefly describes the co-simulation platform developed for simulating the cyber-physical dynamics of the distribution grid and simulating attack scenarios at various parts in the grid. The platform combines various industry-grade and open-source tools such as GridLAB-D, NS3, HELICS to emulate the different layers of the grid infrastructure. The platform uses the communication protocol, DNP3, for the grid communications. This paper focuses on generation of man-in-the-middle attack behavior in distribution grid. We use a Docker container to distribute our tool to other researchers. Docker was chosen since it allows us to create a lightweight environment that can easily be used by other researchers. The container enables researchers that don't have access to an real power network to conduct research on a realistic environment.

#### A. Our co-simulation platform

Our current platform is divided into three layers: the control layer, the network or communication layer, and the physical layer. GridLAB-D is used for the physical layer, while NS3 is used to construct the connecting network. Finally the control layer is represented as the control node and it is controlled through the main simulation program. The control layer consists of one utility control center that receive measurements from and send control commands to the respective microgrids in the physical layer. The network layer represents the communication medium that carries information between the control and the physical layer. This layer consists of various network topology and uses DNP3 as grid communication protocol between the control layer and physical layer.

The physical layer consists of the physical distribution grid using IEEE 123 bus test feeder model with various DERs.

The IEEE 123 bus feeder model is further logically split into three microgrids which can be configured in grid connected or islanded mode. Each microgrid has a substation which have remote terminal units (RTUs) that aggregate data from and disseminate control signals coming from the control center to various DERs in the microgrid. The control center does periodic poll requests every 4 seconds. Once the poll request is received, the microgrid/substation responds with collected measurements. A man-in-the-middle attack node sits between the control center and each of the substations. The man-in-the-middle attacker changes the data that are sent between the substations and the control centers. The attacker's goal is to trick users into thinking the substations sent good data to the control center while sending a different command to the substation. The different command can be used to collect additional information from the substation or modify parameters such as tripping a relay in the microgrid.

1) *GridLAB-D and IEEE 123 node test feeder*: The GridLAB-D simulation tool is used to model the IEEE 123 node test feeder [15]. This test feeder is used as the base power system model for the developed tool and multiple distributed energy resources (DERs) are integrated at different locations to construct a distribution system architecture with three different microgrids. The microgrids can be connected to the grid or islanded in different combinations to create different feeder structures. Each microgrid consists of three DERs: one grid-following inverter based photovoltaics (PV), one grid-connected inverter based PV and one diesel generator. The generator is modeled using synchronous machine with simple excitation system enabling droop curve to the voltage/reactive power output, and GGOV1 governor model with primary power and frequency droop controls. Similarly, inverters are equipped with current and voltage control loops to adjust various droop characteristics, and functions to change active and reactive power and voltage set-points. There are physical and virtual relays with over-current, over-frequency, and under-frequency protection functions integrated in different locations in the test feeder.

2) *HELICS-NS3*: For our platform, as seen in Figure 1, we use HELICS as a interconnecting bridge between GridLAB-D and NS3. At the start of a simulation run, the HELICS-NS3 node and GridLAB-D connect to the HELICS broker as federates and are ready to send/receive data from/to each other. Each NS3 node is assigned a HELICS endpoint that is used to communicate with the HELICS broker. The HELICS broker serves as the timekeeper for the simulation. When the NS3 node receives a data request, it pings the GridLAB-D tool for the updated values for the registered points. Similarly, when the NS3 node receives a control command signal, it converts the command signal to GridLAB-D setpoint change request to the GridLAB-D tool via HELICS broker. Once the request is fulfilled, the broker advances the simulation to the next timestep. This continues until the end of the simulation.

3) *DNP3-NS3*: We added DNP3 protocol into NS3 to simulate realistic grid communication scenarios between utility control center and the distributed grid. The DNP3-NS3 module requires a configuration file consisting of all the measurement data expected from GridLAB-D simulation. The data points

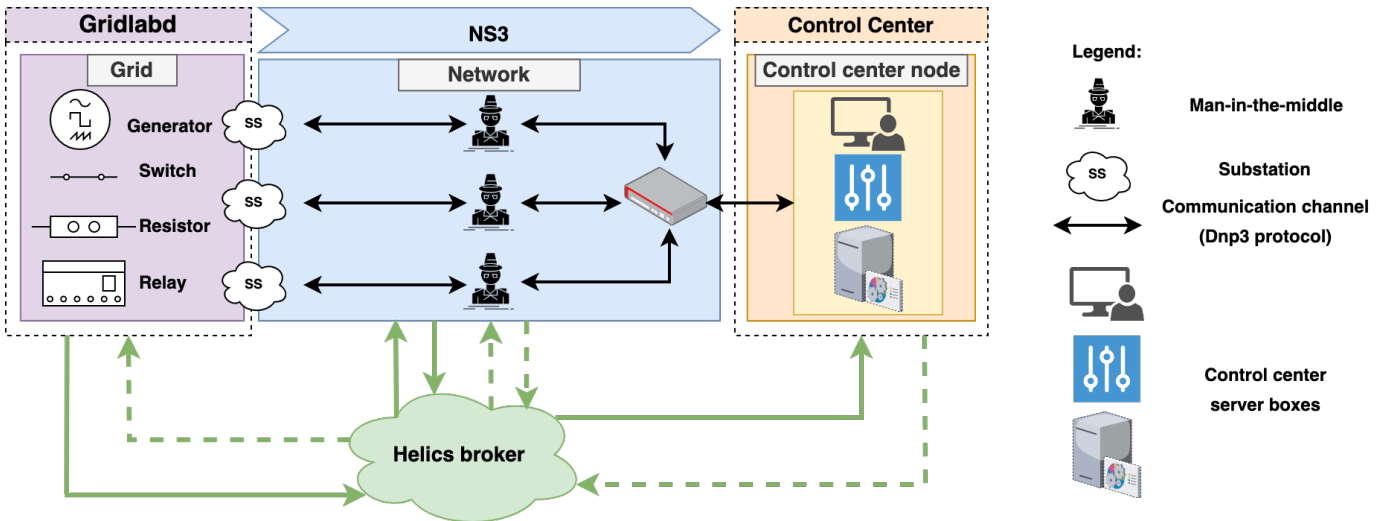


Fig. 1: Overview of the co-simulation environment with interactions between HELICS, GridLAB-D and NS3. Each node uses the DNP3 protocol to communicate. The control center, where the Open Platform Communications (OPC) server is located, is responsible for control a region of the grid network. The substation is responsible for power distribution and aggregating the information for the microgrid to be sent to the control center. The control center does periodic poll requests every 4 seconds. Once the poll request is received, the microgrid/substation responds with collected measurements.

are GridLAB-D specific names of measurement data or set-points such as active power, voltage settings, ON/OFF states of switches etc. configured as analog or binary points. There are other types of points, but we focus on analog and binary points for the scope of this paper. To generate distribution grid scenarios, NS3 node with HELICS-NS3 and DNP3-NS3 modules enabled is needed. At the start of a simulation run, GridLAB-D measurement points get registered with GridLAB-D through HELICS broker. HELICS-NS3 is responsible for retrieving measurements from GridLAB-D tool and sending set-points to modify the DER settings. The DNP3-NS3 module is responsible for converting raw GridLAB-D measurement values into DNP3 protocol format and also translating DNP3 control commands into GridLAB-D specific set-point instructions.

## B. Configurations

1) *Network Topologies*: Our tool takes a JSON file containing node to node connections, gives it to NS3, and uses it to build a topology. Normally, to make sure that the topology is valid, a user can use a topology generator such as NS3 topology generator [25], but doing so requires prior knowledge of operating NS3. We simplify this process by reducing the knowledge needed to operate NS3 to a configuration file, thereby removing the need for additional programs outside the ones already installed in our Docker container.

The configuration file allows control over the jitter of a node, the connection type between two nodes, and the topology of the network. For example, a user can create a configuration that generates a topology where there are two groups of nodes: The first group of nodes is connected using Carrier Sense Multiple Access (CSMA) following a mesh topology structure, and the second group is connected using a point to point connection using a star topology. Then both

of the groups can be connected over Wi-Fi so that data can be sent between each cluster. This example is one of many configurations that can be created.

2) *Cyber-Attack*: We use JSON files to setup the attack in our setup. The configuration file takes in the start and end time of the attack, the number of attackers in the network and attack specific values. The attack-specific values include the parameters of the victim device that are being attacked, such as active or reactive power settings. It also includes the attack value that the attacker uses to update the value of the device parameter. Finally, the user can also select the attack scenario that they want to simulate on the network.

## C. Attack generation method

To generate attacks, we use the internet module and the DNP3 module to intercept a packet and update it to contain new data. If the destination address is found to be the victim address, then the attacker simulates the packet arriving to its original destination. Then, through the DNP3 protocol, the attacker simulates sending a new packet containing the updated information or command. The *CapturePacket* function is set in the ipv4 I3 protocol module. The rest of the functions are developed through the DNP3 module. In Algorithm 1, the packet can be intercepted using the internet stack before it is sent to the target node(s).

1) *Our attacker*: Our attacker is a man-in-the-middle attacker who has access to a network node using a DNP3 application within NS3. The attacker uses a modified ipv4 I3 protocol to identify if the message that is intercepted is heading to the ipv4 address of the victim. Once the victim address is identified, the attacker captures the messages, and sends an updated message with new data in place of the old. Before the message is sent, the source address is updated to match the address of the original sender. Thus, once the receiver gets

---

**Algorithm 1** Packet interception algorithm at the stack. *ContToSub* shows the information flow from control center to the substation. *SubToCont* shows the information flow from the substation to the control center.

---

```

1: victimAddr  $\leftarrow$  Address of the victim node
2: IsDestination  $\leftarrow$  False
3: function CAPTUREPACKET(p, addr)
4:   if addr = victimAddr then
5:     IsDestination  $\leftarrow$  True
6:   end if
7: end function
8: function CONTTOSUB(AppHeader ActionID, UserData
  data, AppSeqNum seq)
9:   packet  $\leftarrow$  initiateReq(ActionID);
10:  transmit(packet, data, seq)
11: end function
12: function SUBTOCONT(UserData data, map  $<$ 
  string, float  $>$  analog_points, map  $<$ 
  string, uint_t  $>$  bin_points, AppSeqNum seq)
13:   for k in analog_points do
14:     packet  $\leftarrow$  k
15:   end for
16:   for k in bin_points do
17:     packet  $\leftarrow$  k
18:   end for
19:   transmit(packet, data, seq)
20: end function
21: function SENDNEWPACKET(DestID, SrcID)
22:   if IsDestination then
23:     UserData data.dest  $\leftarrow$  DestId
24:     UserData data.src  $\leftarrow$  SrcId
25:     AddSeqNum seq  $\leftarrow$  current sequence number
26:     map  $<$  string, float  $>$  analog_points  $\leftarrow$  up-
  dated analog points
27:     map  $<$  string, uint16_t  $>$  bin_points  $\leftarrow$  up-
  dated binary points
28:   end if
29: end function

```

---

the message, they will act upon it as if it was from a legitimate source. The attack can be used as a standalone attack where the goal is to spread misinformation; or it can be used as a part of a larger attack where the goal would be not only to spread misinformation but also to take control over a node/section of the network.

For this attack scenario, the attacker intercepts traffic going from the control center to the substation or the microgrid or from the substation to the control center. When intercepting the packet going from the control center to the substation, the attacker modifies the packet to not only conduct the normal action that was requested from the control center but to also conduct an action chosen by the attacker. For example, if the control center sends out a poll request to the individual nodes in the network, the attacker can intercept that message and send an action to the recipient to trip a relay and modify the resulting data that is returned by the substation to hide the changed values. By intercepting the data going from the

---

**Algorithm 2** DNP3 packet update.

---

```

1: AttackValues  $\leftarrow$  Updated values the attacker uses
2: PointIDs  $\leftarrow$  Point IDs that are attacked
3: NodeIDs  $\leftarrow$  Node IDs that are attacked
4: function GETINDEX(NodeID+PointID)
5:   for k in analog_points do
6:     if k = NodeID + PointID then
7:       return index of k
8:     end if
9:   end for
10:  for k in bin_points do
11:    if k = NodeID + PointID then
12:      return index of k
13:    end if
14:  end for
15: end function
16: function SENDACTION(AttackValues, PointIDs, NodeIDs)
17:   for k in PointIDs and c in NodeIDs do
18:     index  $\leftarrow$  GetIndex(c + k)
19:     UpdatePointValue(index)
20:   end for
21:   ForwardPollRequest()
22: end function

```

---

substation to the control center, the attacker can send fake data to the control center as an attempt to trick the control center into thinking that everything is fine at the substation level.

#### IV. EXPERIMENTAL SETUP

This section describes generation of three types of attack scenarios on a distribution grid. We also demonstrate how to use our tool to modify where the attacker is and how the attack impact varies depending on the location of the attacker in the network. For all of the three attack scenarios described below, the attacker is located between the control center and the substation.

- In the first attack, the attacker intercepts the measurement data flowing from substation to control center and modifies the reactive power setpoints/reference (Qref) of Inverter 42 (grid-following inverter) situated in Microgrid 1.
- In the second attack, the attacker intercepts the DNP3 command flowing from control center to the substation and modifies the active power setpoints (Pref) value for both grid-following and grid-forming inverters -Inverter 42 and Inverter 51 of Microgrid 1. Additionally, during both of these attacks the switches connecting the microgrids are tripped to island the microgrids from each other and the grid.
- In the third attack, the attacker intercepts the DNP3 command flowing from control center to the substation and islands the microgrids from each other and the grid. We conduct that attack to examine the impact of an islanding attack on the frequency measured on Microgrid 3. Islanding happens when microgrids are disconnected from one another, making the microgrids dependent on

their individual power sources. Finally, once we find a set of parameters that can be used to counter the effect of islanding on the frequency, we trip an internal virtual relay to cause extra load shedding.

- In the fourth attack, the attacker is in the same location as with attack 2 and 3. We conduct the two previous attacks on a ring topology. The attacks in the previous scenarios were conducted in a star topology. The goal of this attack is to compare the effect of both attacks on the analog and binary points that are sent from the substation to the control center on a different topology.

#### A. Data format and setup

The experiment setup has a control center that is responsible for monitoring the distribution grid of an area. The grid consists of the IEEE 123 test feeders with three microgrids. The grid dynamics is simulated using GridLAB-D tool. The microgrids can be islanded by tripping the relay/switches connecting them to each other and the grid. Each microgrid has a substation which acts as the remote terminal units (RTUs) that aggregate data from and disseminate control signals coming from the control center to various DERs in the microgrid. The control center and substation are setup as NS3 nodes and communicate over virtual NS3 network. The substation nodes have HELICS-NS3 to integrate with GridLAB-D. The control center and substations have DNP3-NS3 module installed to provision DNP3 based grid communication. The control center makes a periodic DNP3 polling request (every 4 seconds) to each of the substations for latest measurement values from the microgrid. Each of the substations respond back with data collected from GridLAB-D simulation for the respective microgrid. The control center can also send DNP3 control command to a substation to control a particular set-point of DER in the microgrid. The substation acts on the control command by sending write instruction to the GridLAB-D simulation.

During the configuration setup, all the GridLAB-D specific measurement data such as active power, reactive power, ON/OFF state of switches are pre-configured as DNP3 analog and binary points in a configuration file. During simulation start-up, these data points are ingested by NS3-HELICS module at the substation node and registered with GridLAB-D. The raw measurements are collected and converted into DNP3 protocol format. The packaged data is then sent to the control center for processing over the network.

Figure 2 shows the system architecture with the design of our power grid, and the grid consists of the IEEE 123 test feeders with three microgrids. The microgrids can be islanded by tripping the relay/switches connecting them to each other and the grid. The control center and the substation are also connected to the router where NS3 is loaded to allow different topologies during experimentation.

#### B. Topologies tested

We run our attacks on two topologies: a default star topology that has the control center at the center of the network and

a ring topology built using our topology configuration file. Figure 3 illustrates both of the topologies.

#### C. Attack scenarios

We place an attacker located between the control center and the microgrid/substation. The attacker must stay unnoticed since it does not have authority to be on the network. Using a modified Internet Stack, the attacker reads the bytes in the packet and, if it finds a certain packet that matches the requirement for the attack, executes an interception. The attacker then modifies the intercepted packet data to communicate false information to the control center. This attack can be also used in conjunction with a command injection. Using both, an attacker can perform changes to the settings of a node while hiding it from the control center.

1) *Attack 1: Data Modification:* In this scenario, the attacker intercepts a poll request response going from the substation to the control center. The attacker then modifies the reactive power setpoints/reference (Qref) of Inverter 42 (grid-following inverter) situated in Microgrid 1 to trick the control center to believing that the inverter is in a different state than its current state.

2) *Attack 2: Inverter active/reactive power setpoints modifications:* In this scenario, the microgrids are islanded from other microgrids and the grid. Then, a man-in-the-middle (MITM) attack changes the setpoint of an inverter to introduce voltage issues. The attack happens at approximately two minutes into simulation. As seen in Table I, Inverter 42 has its Qref setpoint changed from 0 Var (default) to  $-50$  kVar (attack value). In the second scenario, the microgrids are also islanded. Then, inverters are attacked consistently to cause voltage stability issues: Inverter 42 has its Pref value randomly toggled between 450 kW (default) and 350 kW (attack value) and Inverter 51 has its Pref value randomly toggled between 210 kW (default) and 110 kW (attack value). The attack starts at approximately two minutes into simulation.

This scenario uses packet capture (PCAP) files that are generated by NS3 to identify the attack and quantify its impact on the resulting network. PCAP files are used as ways to visualize network traffic. NS3 can generate them using the point to point helper class in the point to point module and can be read using Wireshark.

3) *Attack 3: Tripping relays using command injection:* In this scenario, a command injection attack causes islanding of microgrids, as shown in Table II. In some cases, power generation is enough to sustain the loads running on the microgrid, while in others (i.e. Microgrid 3) limited power generation increases the Under-Frequency-Load-Shedding (UFLS). UFLS occurs due to insufficient generation on the microgrids to supply the load. The sw60to160 relay was tripped via command injection at approximately two minutes into data capture. In another version of this attack, power dispatch has been adjusted to minimize UFLS. Finally in a third version of this attack, the sw60to160 relay is tripped and the config file of the sw76to86 virtual relay was modified so that additional UFLS would occur.

For this experiment, we use frequency measurement to compare the three parts. Frequency has been used to identify

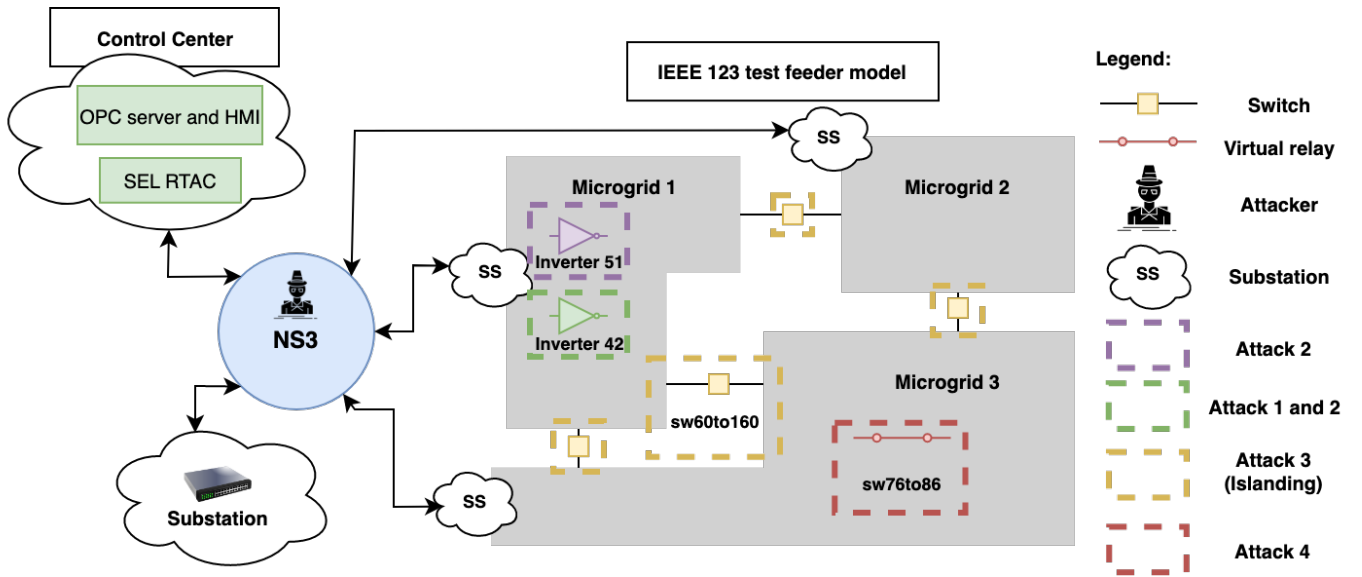


Fig. 2: Microgrid setup for experimentation, using the IEEE feeder model as described by Ashok *et al.* [8]. We use this setup to run the cyber attacks and collect data on how the attacks impact the performance of the power grid. The attack conducts a man-in-the-middle attack on two inverters in Microgrid 1, the switches connecting the Microgrids and the relay in Microgrid 3. Substations can be responsible for power distribution over multiple Microgrids as well as act as aggregate points.

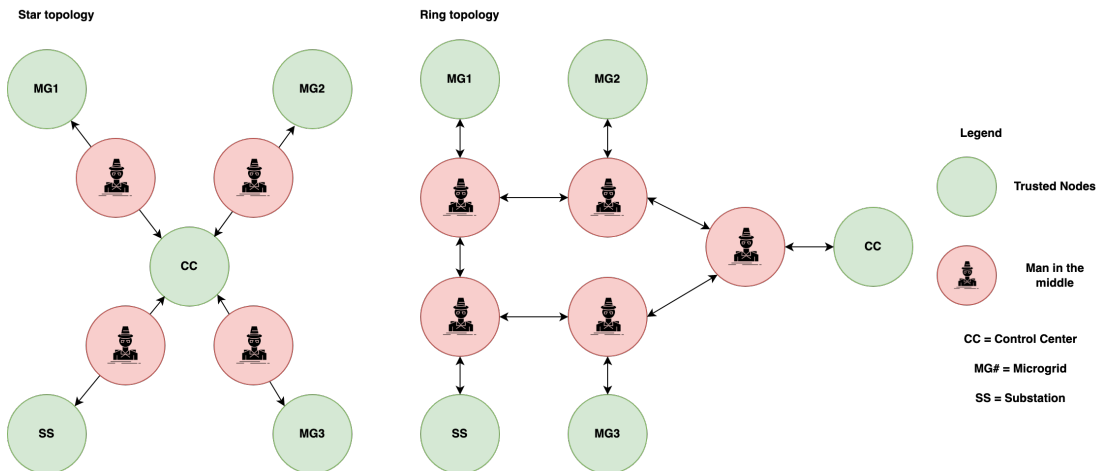


Fig. 3: A simplified presentation of the topologies used in our experiments. The Ring topology was defined using our topology configuration file while the star topology was defined directly in our code as the default topology in case the user does not have a specific topology to use.

any load mismatches that may be happening in a power system [26], [27]. When a cyberattack occurs, its impact on the point value of nodes in a power system causes the frequency to shift away from its normal, pre-attack, value.

#### D. Attack 2 and 3 on a Ring topology

For this scenario, we run attack scenario 2 and 3 on a ring topology. This scenario serves as an example of how to use the dynamic topology configuration function of our tool. We compare the resulting effect of the attack on the collected analog and binary points collected over the grid.

## V. RESULTS

During experimentation, we collect information described in the previous section to demonstrate the operation of our tool. We identified how changing certain parameters, such as the active power of an inverter ( $P_{ref}$ ) value changes, can cause a grid following and grid forming inverter to have different output voltage behavior. Additionally, when looking at the microgrid's frequency change during an attack, by changing the generator's nominal and output power, the frequency was able to return to its value before the attack started.

#### A. Attack 1: Data Modification

We start the experiment by examining the response that is sent from the substation to the control center in response

Inverter Description						
Inverter ID	location	type	Rated	Pref	Qref	attacked values
Inverter 51	MG1	grid forming	400 kW	210 kW	0 VAR	Pref (110 kW)
Inverter 42	MG1	grid following	600 kW	450 kW	0 VAR	Pref (350 kW), Qref (-50 kVAR)
Inverter 101	MG2	grid following	180 kW	126 kW	0 VAR	NA
Inverter 105	MG2	grid forming	600 kW	300 kW	0 VAR	NA
Inverter 76	MG3	grid following	120 kW	84 kW	0 VAR	NA
Inverter 80	MG3	grid forming	100 kW	70 kW	0 VAR	NA

TABLE I: Available Inverters in our current simulation with default and attack values.

Relay Description				
Relay/switch ID	location	type/use	default value	attacked value
sw6to160	grid-MG2	Breaker/Switch	close	open
sw18to135	grid-MG1	Breaker/Switch	close	open
sw97to197	MG2-MG3	Breaker/Switch	close	open
sw54to94	grid-MG3	Breaker/Switch	close	open
sw15to300	MG1-MG2	Breaker/Switch	close	open
sw76to86	MG3	Virtual Relay	close	open

TABLE II: List of relays connecting the microgrids to one another and to the grid. These relays are used in our experiment to island the microgrids from one another. The Virtual Relay is used as a load disconnect to cause additional Under-Frequency-Load-Shedding.

to a poll request. The substation's response is sent in three segments of 274 bytes. This response message contains points, each point representing a value associated with a node. These node points, and their values, represent the behavior of that node at the time the packet was sent, for example, the output voltage of generator 1. Each of these points are separated by a flag, and the flag represents whether or not that point was set correctly.

An attacker who has access to these response packets can use a history of these packets to build an understanding of what nodes constitute the microgrid. For this experiment, we intercept some of these response packets, and change several points inside them, as seen in Figure 4. After the bytes are updated by the attacker, the attacker sends out the updated packet with the new values back into the network. Our tool can generate PCAP files through the NS3 simulator, which can be used to visualize this attack.

### B. Attack 2: Inverter active/reactive power setpoints modifications

The attacker starts by reducing the Qref value of inverter 42 two minutes into the simulation, as seen in Figure 6. This causes a slight decrease in current, as seen in Figure 5 where the current normally averages between 7359 W to 7346 W. This very slight increases in maximum and decreases in minimum, resulting in larger waves, in current may go unnoticed if there is no existing knowledge that a change similar to this observed change signifies an adversary on the network. Reactive power (Qref) maintains voltage levels that are needed for system stability. Therefore, it makes sense that by reducing the Qref value, the current value changes over time.

Our tool can visualize these changes to make informed decisions on how they can tackle such attacks. A user can use the datasets generated by our tool to train models to identify

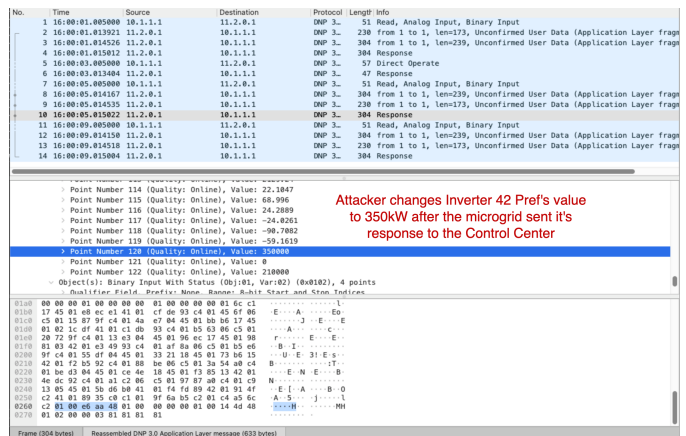


Fig. 4: The attacker modifies the response from the substation to the control center to make the control center believe that the Pref value of inverter 42 is set to 350 kW instead of 450 kW, its default value.

and counter attackers based on the impact that is viewed at the node level. In this case, if an inverter's current suddenly drops, the traffic can be rerouted away from that inverter and microgrid to isolate that section of the network. Additionally, the network can send a signal that a section of it is under attack so that some countermeasure can be applied to eliminate the threat.

Our tool can also be used to simulate a multi-node attack, as demonstrated in the second part of this attack. Here, the attacker randomly varies the Pref value of two inverters on Microgrid 1 as seen in Figure 7.

Figure 8 shows a drastic decrease in output voltage of Inverter 42 during the attack where the attacker randomly increases and decreases the Pref value. As seen in Figure 7, the variation in Pref value matches the variation in output voltage



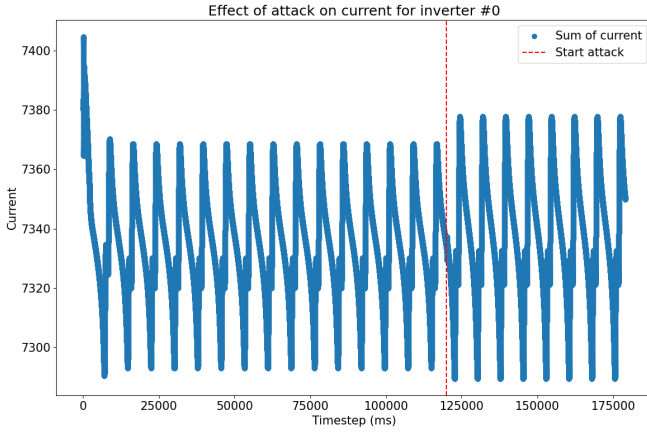


Fig. 5: Current change once the attack starts at load 42, which is the load connected to inverter 42. The attack starts 2 minutes in the simulation and causes a shift in the current fluctuation of the load, where the current waves became bigger compared to before the attack.

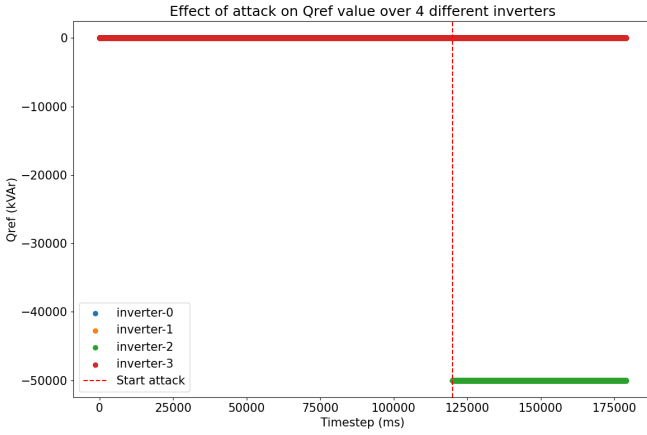


Fig. 6: The  $Q_{ref}$  of inverter 42 (inverter-2) is dropped to  $-50$  kVAR from  $0$  kVAR (the default value) after 2 minutes in the simulation. The rest of the inverters are not attacked.

for inverter 42 (inverter-2). The output voltage drops to the attack value of  $350$  kW when the attacker sets the  $P_{ref}$  value to  $350$  kW. By identifying these drop in voltages, a user of our tool can create counter measures to such attacks by potentially resetting the inverter if the voltage fluctuates erratically.

Figure 9 shows how the attack happening on Microgrid one's inverter can affect the resulting output voltage in inverters in a separate microgrid. Since Microgrid 1 is islanded from the rest of the Microgrids and the grid when the attack starts, we can observe an increase in power fluctuation when looking at the output voltage of the inverters.

Figure 10 shows the impact of the attack on a grid forming inverter. In this case, we can see a significant drop in the inverter's output voltage, but it is quickly brought back to its normal value after a few timesteps. The fluctuations observed in Figures 8 and 10 show that a grid forming inverter is less susceptible to attacks on the  $P_{ref}$  value compared to a grid following inverter.

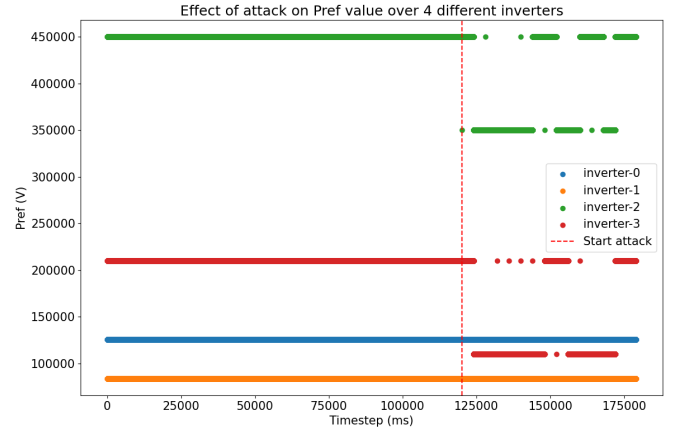


Fig. 7: The  $P_{ref}$  of Inverter 42 (inverter-2) is dropped to  $350$  kW from  $450$  kW (the default value) and the  $P_{ref}$  value of Inverter 51 (inverter-3) is dropped from  $210$  kW to  $110$  kW after two minutes in the simulation. This is an example of the  $P_{ref}$  values being randomly fluctuating between the default and attack values.

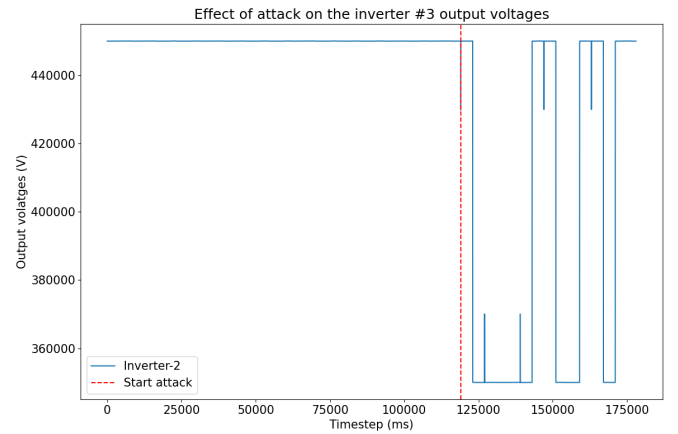


Fig. 8: Effect of attack on inverter 42's, a grid following inverter, output voltage. The attacker dynamically fluctuates the  $P_{ref}$  value of two distinct inverters to affect the resulting output voltage and current of the microgrid. In this scenario the microgrids are islanded from both each other and the grid.

We can also visualize the attacks with PCAP files. Figure 11 shows how the  $P_{ref}$  value changes over time. Using PCAP, we can see the cycle of commands that is sent by the attacker to the inverter. We can also see that the only points that get modified are the  $P_{ref}$  value of both of the inverters. Interestingly, the size of the packet that is received as a response from the microgrids varies between  $230$  Bytes and  $304$  Bytes as the  $P_{ref}$  fluctuates. This is another indication that can be used by a user to identify an attacker on the system.

### C. Attack 3: Tripping relays using command injection

In this scenario, we are trip the relays connecting the microgrids to one another, as seen in Table II. We look at the frequency measurement of the microgrids to identify how

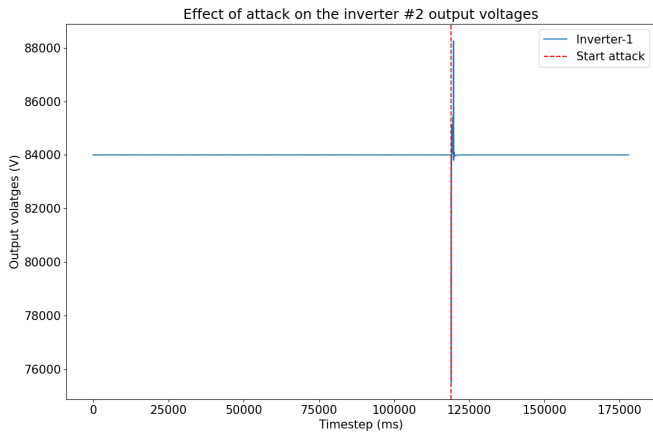


Fig. 9: Impact of attack on inverter 42 and inverter 51 on an inverter's output voltage in a different microgrid

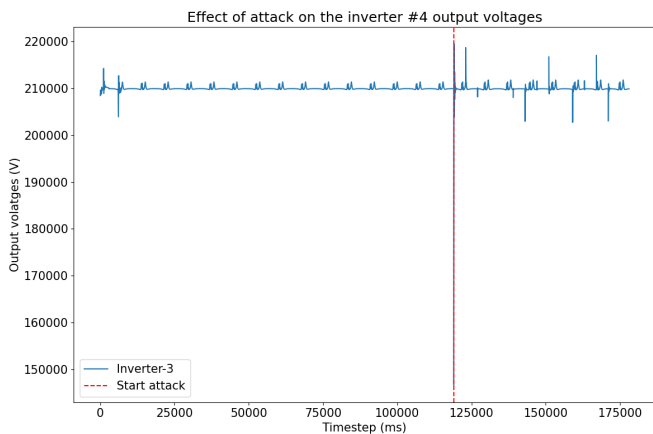


Fig. 10: Impact of attack on inverter 51's, a grid forming inverter, output voltage

resilient it is to attacks. Tripping the relays can cause the microgrids to become islanded from one another and the grid. Notably in this attack, microgrid 3, as shown in Table III, is the only microgrid that has capacitors and it contains one large capacitor connected to multiple phases and three smaller capacitors connected to individual phases. In Figure 12, we can see that the frequency of the attacked microgrid increases to around 71 Hz during scenario A, the scenario where the generator and capacitor use the default value for our tool, as seen in Table IV. Out of all the Microgrids, Microgrid 3 has the lowest power generation, causing it to struggle if Microgrid 3 is islanded, such as the result of tripping the relays in this attack.

Capacitors are a useful tool when regulating the frequency of a microgrid during an attack. When the simulation ran with a larger capacitor and a generator with a lower nominal power rating and lower power amount delivered to interconnected nodes, as seen in Table V, the frequency returns to the normal pre-attack value after approximately two minutes.

Finally, when we trip the virtual relays between nodes 76 and 86, as seen in Figure 2, while keeping the changes created in scenario B, we can see that the frequency does not return to

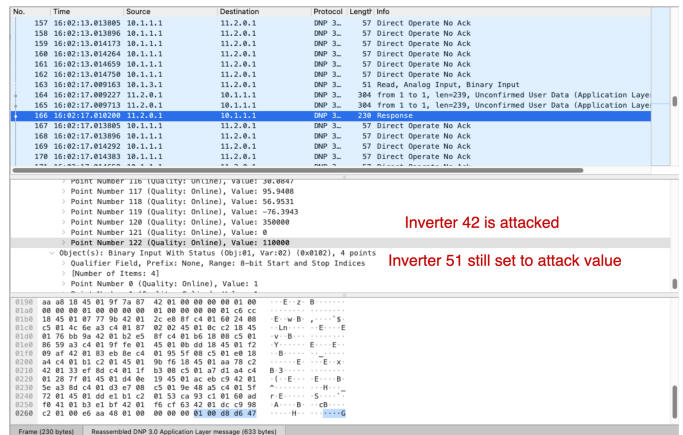
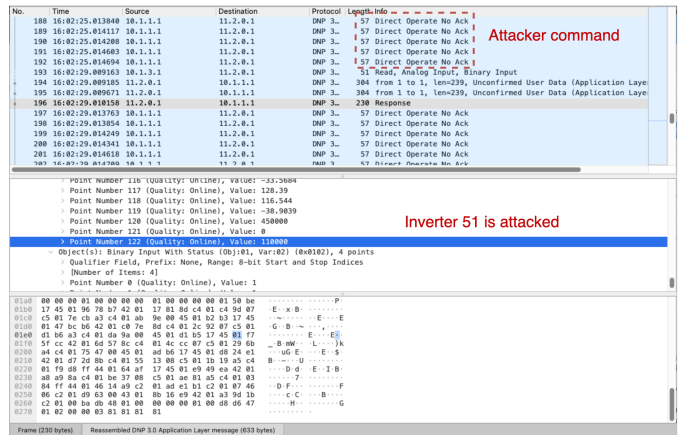
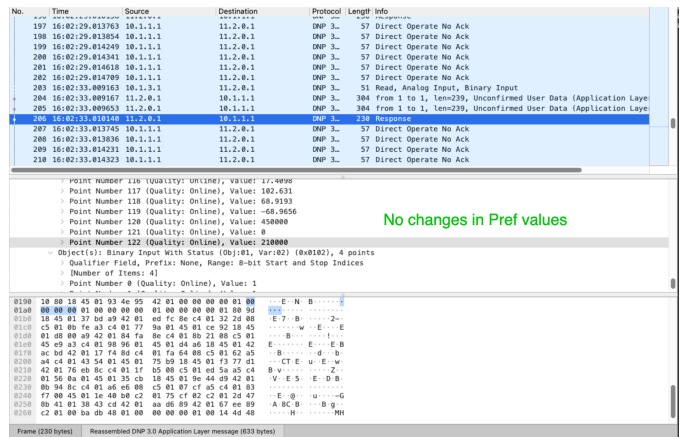


Fig. 11: Visualization of attack through PCAP file.

the value before the attack started. Additionally, the frequency does not drop as much as during the scenario A attack. We also observe that after an initial climb, the frequency slightly drops before starting to climb at a slower rate. The frequency finally stabilizes at around 140 seconds.

#### D. Attack 2 and 3 on a Ring topology

Using our topology configuration file, we change the resulting topology from a star topology to a ring topology, as seen in Figure 3. Each substation/microgrid/control center node is connected to a ring of intermediate nodes. The nodes on the

Microgrid 3 Capacitor Default values			
ID	phases	Nominal power	Capacitor size information
cap83	A, B, C	2401.7771 V	A=200 kVAr, B=200 kVAr, C=200 kVAr
cap88	A	2401.7771 V	A=50kVAr
cap90	B	2401.7771 V	B=50kVAr
cap92	C	2401.7771 V	C=50kVAr

TABLE III: Microgrid 3 is the only microgrid containing capacitors. The size information is in regard to the capacitor size that is connected to a specific phase. For example, in this table, A=200 kVAr represents the size of the capacitor connected to phase A.

Synchronous Generator Default values			
ID	location	rated power output	power delivered to inter-connected nodes
Gen1	MG1	10 MW	30 kW+3000 j
Gen2	MG1	1 MW	25 kW+8333 j
Gen3	MG3	450 kW	50 kW+16667 j
Gen4	MG2	600 kW	50 kW+16667 j

TABLE IV: GridLAB-D simulates 2 types of generators (synchronous vs induction). The microgrids only use synchronous generators. Microgrid 3's generator is rated with the lowest power level out of the rest of the generators. It also delivers the most (tied with Gen4) power to the interconnected nodes.

Updated Generator and Capacitor values			
ID	location	rated/Nominal power	delivered power/capacitor size
cap83	A, B, C	2401.7771 V	A=600 kVAr, B=600 kVAr, C=600 kVAr
Gen3	MG3	300 kW	20 kW+16667 j

TABLE V: All three phases are increased to 600 kVAr. Both the rated and delivered power for Generator 3 are reduced for this part of the experiment.

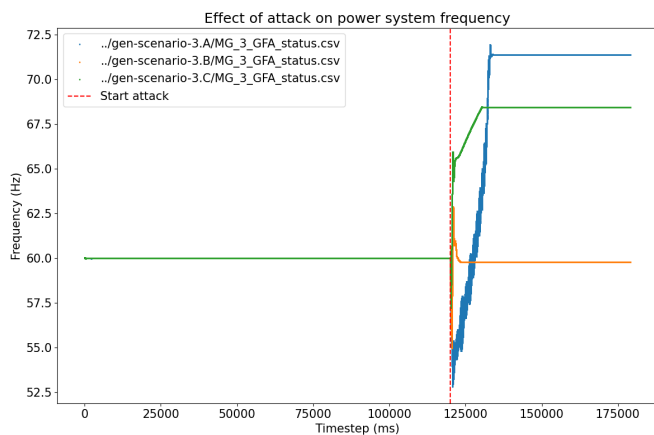


Fig. 12: Frequency changes depending on when the attack starts and what changes, if any, are done to reduce the frequency deviation.

ring are then used to conduct the man-in-the-middle attack. We conduct the same attack as in the previous section where we modify the Pref and Qref value of two different inverters located on the same microgrid. For this topology, similar to the previous topology, the nominal power was only lowered to 300 kW. Using our tool, we found out that to mitigate frequency changes when Microgrid three is islanded the same parameter values for the generator and the capacitor worked for both the ring and star topology.

With regards to attack 2, where the Qref and Pref values are modified, we can observe that on this topology, when the Qref

or Pref values are lowered, that the resulting current measured at the inverter fluctuates more similar to what was observed in a star topology. Figure 13 shows the resulting current measured at the connected load to inverter 42 in Microgrid 1 when the Pref value for both inverter 42 and 51 have their Pref value fluctuating over time. We can see that the waves have both a smaller minimum and a higher maximum similar to the current graph for the star topology.

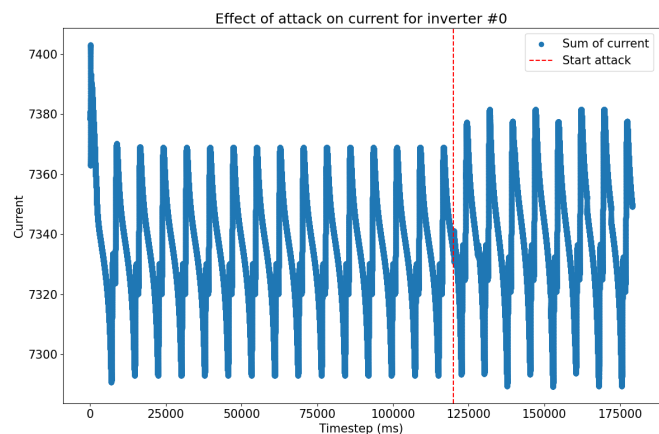


Fig. 13: Current change once the attack starts at load 42, which is the load connected to Inverter 42 when the Pref value of both Inverter 42 and 51 are fluctuating. The attack starts 2 minutes into the simulation and causes a shift in the current values of the load.

## VI. CONCLUSION AND FUTURE WORK

We demonstrate the benefit of using a lightweight tool to model different security scenarios and their effect on grid nodes. We also described the design of our tool, and how it uses the IEEE model from GridLAB-D to model grid components. Using our tool, we identified that there is differing behavior between grid forming and grid following inverters when the Pref and Qref values are changed by an attacker. Grid following inverters are more affected by any changes done to the Pref value, while grid forming inverters can restabilize the output voltage of the inverter down to its original value. We also identified parameter settings that enable the microgrid to recover the original frequency value once the microgrid is islanded.

In future work, we will implement insider attacks as part of our simulation tool. This attacker takes over a trusted and authorized node in the network and intercepts traffic going both directions between the substation and the control center. The attacker can inform the control center that the substation is working properly while conducting a denial of service attack, for example. This attack effectively renders the attacker's action invisible to the control center. By the time the attack is detected, the attacker could have stolen private information or destabilized part(s) of the system.

In addition, we will expand the capability of topology configuration files. We will also add the ability to enable neural network control routing decision to optimize different performance values of the network. We will add the ability to set the protocol used for communication as well as the type of connections, such as point to point, CSMA connections, and/or LTE/DNP3 protocols. Finally we will make our tool publicly available as a docker container.

## ACKNOWLEDGMENTS

We would like to thank Md Touhiduzzaman and Burhan Hyder for their valuable feedback on the paper.

## REFERENCES

- [1] A. Lee, "Electric sector failure scenarios and impact analyses-version 3.0," *Electric Power Research Institute, Palo Alto, CA*, 2015.
- [2] A. Dutta, S. Purohit, A. Bhattacharya, and O. Bel, "Cyber attack sequences generation for electric power grid," in *2022 10th Workshop on Modelling and Simulation of Cyber-Physical Energy Systems (MSCPES)*, pp. 1–6, IEEE, 2022.
- [3] I. Zografopoulos, J. Ospina, X. Liu, and C. Konstantinou, "Cyber-physical energy systems security: Threat modeling, risk assessment, resources, metrics, and case studies," *IEEE Access*, vol. 9, pp. 29775–29818, 2021.
- [4] A. Bhattacharya, T. Ramachandran, S. Banik, C. P. Dowling, and S. D. Bopardikar, "Automated adversary emulation for cyber-physical systems via reinforcement learning," in *2020 IEEE International Conference on Intelligence and Security Informatics (ISI)*, pp. 1–6, IEEE, 2020.
- [5] L. Barnett III, "Netsim: a network performance simulator," 1992.
- [6] B. Lantz, B. Heller, and N. McKeown, "A network in a laptop: rapid prototyping for software-defined networks," in *Proceedings of the 9th ACM SIGCOMM Workshop on Hot Topics in Networks*, pp. 1–6, 2010.
- [7] D. Lee, H. Kim, K. Kim, and P. D. Yoo, "Simulated attack on dnp3 protocol in scada system," in *Proceedings of the 31th Symposium on Cryptography and Information Security, Kagoshima, Japan*, pp. 21–24, 2014.
- [8] A. Ashok and T. Edgar, "A high-fidelity cyber-physical testbed-based benchmarking dataset for testing operational technology specific intrusion detection systems," in *2021 IEEE International Symposium on Technologies for Homeland Security (HST)*, pp. 1–7, IEEE, 2021.
- [9] A. Dabrowski, J. Ullrich, and E. R. Weippl, "Grid shock: Coordinated load-changing attacks on power grids: The non-smart power grid is vulnerable to cyber attacks as well," in *Proceedings of the 33rd Annual Computer Security Applications Conference*, pp. 303–314, 2017.
- [10] S. Aoufi, A. Derhab, and M. Guerroumi, "Survey of false data injection in smart power grid: Attacks, countermeasures and challenges," *Journal of Information Security and Applications*, vol. 54, p. 102518, 2020.
- [11] R. V. Yohanandhan, R. M. Elavarasan, P. Manoharan, and L. Mihet-Popa, "Cyber-physical power system (cpps): A review on modeling, simulation, and analysis with cyber security applications," *IEEE Access*, vol. 8, pp. 151019–151064, 2020.
- [12] G. Carneiro, "Ns-3: Network simulator 3," in *UTM Lab Meeting April*, vol. 20, pp. 4–5, 2010.
- [13] D. P. Chassin, K. Schneider, and C. Gerkensmeyer, "Gridlab-d: An open-source power systems modeling and simulation environment," in *2008 IEEE/PES Transmission and Distribution Conference and Exposition*, pp. 1–5, IEEE, 2008.
- [14] B. Bhattarai, L. Marinovici, M. Touhiduzzaman, F. K. Tuffner, K. P. Schneider, J. Xie, P. Thekkumparambath Mana, W. Du, and A. Fisher, "Studying impacts of communication system performance on dynamic stability of networked microgrid," *IET Smart Grid*, vol. 3, no. 5, pp. 667–676, 2020.
- [15] K. P. Guddanti, Y. Ye, P. Chongfuangprinya, B. Yang, and Y. Weng, "Better data structures for co-simulation of distribution system with gridlab-d and python," in *2020 IEEE Power & Energy Society General Meeting (PESGM)*, pp. 1–5, IEEE, 2020.
- [16] P. T. Mana, K. P. Schneider, W. Du, M. Mukherjee, T. Hardy, and F. K. Tuffner, "Study of microgrid resilience through co-simulation of power system dynamics and communication systems," *IEEE Transactions on Industrial Informatics*, vol. 17, no. 3, pp. 1905–1915, 2020.
- [17] I. A. Siddavatam and F. Kazi, "Security assessment framework for cyber physical systems: A case-study of dnp3 protocol," in *2015 IEEE Bombay Section Symposium (IBSS)*, pp. 1–6, IEEE, 2015.
- [18] S. East, J. Butts, M. Papa, and S. Shenoi, "A taxonomy of attacks on the dnp3 protocol," in *International Conference on Critical Infrastructure Protection*, pp. 67–81, Springer, 2009.
- [19] V. Kumar, S. Chakraborty, F. A. Barbhuiya, and S. Nandi, "Detection of stealth man-in-the-middle attack in wireless lan," in *2012 2nd IEEE International Conference on Parallel, Distributed and Grid Computing*, pp. 290–295, IEEE, 2012.
- [20] R. Liu, C. Vellaithurai, S. S. Biswas, T. T. Gamage, and A. K. Srivastava, "Analyzing the cyber-physical impact of cyber events on the power grid," *IEEE Transactions on Smart Grid*, vol. 6, no. 5, pp. 2444–2453, 2015.
- [21] M. Apriani, D. Rousstia, F. A. Rifai, R. Harwahu, and R. F. Sari, "Implementation of secure work from home system based on blockchain using ns3 simulation," in *2020 7th International Conference on Electrical Engineering, Computer Sciences and Informatics (EECSI)*, pp. 54–59, IEEE, 2020.
- [22] M. N. Mejri, N. Achir, and M. Hamdi, "A new group diffie-hellman key generation proposal for secure vanet communications," in *2016 13th IEEE annual consumer communications & networking conference (CCNC)*, pp. 992–995, IEEE, 2016.
- [23] C. Devanarayana, Y. Zhang, and R. Kuffel, "Testing cyber security of power systems on a real time digital simulator," in *2019 IEEE 8th International Conference on Advanced Power System Automation and Protection (APAP)*, pp. 1166–1170, IEEE, 2019.
- [24] S. P. Nandanoori, "Nominal and adversarial synthetic pmu data for standard ieeec test systems," tech. rep., Pacific Northwest National Lab.(PNNL), Richland, WA (United States), 2021.
- [25] R. Halder, S. Mundra, U. Dey, S. Ghosh, S. Karmakar, and R. Karmakar, "Ns3tcg: Ns3 topology and code generator," in *2018 International Conference on Recent Innovations in Electrical, Electronics & Communication Engineering (ICRIEECE)*, pp. 865–870, IEEE, 2018.
- [26] T. Lobos and J. Rezmer, "Real-time determination of power system frequency," *IEEE Transactions on Instrumentation and Measurement*, vol. 46, no. 4, pp. 877–881, 1997.
- [27] J.-Z. Yang and C.-W. Liu, "A precise calculation of power system frequency," *IEEE Transactions on Power Delivery*, vol. 16, no. 3, pp. 361–366, 2001.